Robotica (1999) volume 17, pp. 79–86. Printed in the United Kingdom © 1999 Cambridge University Press

Wall-following by an Autonomously Guided Vehicle (AGV) Using a New Fuzzy-I (Integration) Controller

Qing-hao Meng*, Da-wei Liu**, Ming-lu Zhang* and Yi-cai Sun*

(Received in Final Form: March 23, 1998)

SUMMARY

In this paper, the wall-following problem of an AGV is characterized by keeping a constant distance from a wall. Four Polaroid ultrasonic range sensors (sonar) are used to obtain information of the distance between the AGV and the wall. Four sonars are divided into two groups being placed at the front and back end on the right side of the AGV, respectively. A digital filter is used to get rid of disturbance and wrong readings. The former results mainly from the door and the latter from the specular reflection and accidental scattering. To obtain good dynamic and steady performances, a new compound fuzzy-I control algorithm is presented. Our methods have been verified by following a 15-meter-long wall with one door by using our TIT-1 AGV (TIT: Tianjin Institute of Technology). The results show a good performance with an error of ±2 cm from the desired distance to the wall.

KEYWORDS: AGV; Sonar; Wall-following; Digital filter; Fuzzy-I control

I INTRODUCTION

The AGV is usually applied for transport in structured environments (transport robots in CIMS[1] and service robots in hospitals[2] for example). In such indoor environments, long walls are the main features; thus we believe that following the wall using an AGV is a simple and useful navigation method without modifying the environment. The AGV cannot keep a constant distance from the wall when it begins to move, owing to wheel slip, misalignment and other reasons. Mark B. Kadonoff[3] has described a position estimation method by using a wall-following controller. A circular array of 24 Polaroid sonars has been used to measure the range and bearing to the wall. P. Van Turennount and G. Honderd[4] have also discussed the wall-following problem and developed a simple feedback controller. Their interest is to make a mobile robot keep a trajectory parallel to the wall.

In this paper, the wall-following problem is characterized by maintaining a constant distance from a wall. Only four Polaroid sonars have been used in our experiments to measure the distance between the AGV and the long wall (can also be reduced to two sonars). One of the shortcomings of sonars is the specular reflection from smooth planes. To obtain reliable distance readings, a digital filter is used to get rid of the disturbance from the door and wrong readings from the specular reflection and accidental scattering. A new fuzzy-I controller is used to obtain good dynamic and steady performances. The fuzzy controller consists of three kinds of fuzzy inference rules, which are used to adjust three kinds of moving states of the AGV. When the average reading of one end is larger than the expected distance and that of another end is smaller than the expected one, at the same time, the difference between the average readings of two ends is very small (±4 centimeters in our experiments); the I algorithm is used to eliminate remaining erorrs. High precision (the control errors are ±2 cm) and rapid reaction are the main merits of our control method, which are suitable for the wall-following problem.

* Hebei University of Technology, 300130, Tianjin, (P.R. China)
** Intelligent Machine Institute, Tianjin University, 300072, Tianjin, (P.R. China)

II THE SIMPLE STRUCTURE AND THE KINEMATICS MODEL OF THE TIT-1 AGV

TIT-1 AGV has two back driving wheels and two front castors; the dimensions of the AGV are shown in Fig. 1 (the unit is mm). Two back wheels are driven by two alternating current servo motors; each motor and each back wheel form a closed velocity loop. The linear velocity and angular velocity of the AGV are controlled by adjusting rotational speeds of two driving wheels. The relation between the input voltage of the motor and the rotational speed of the driving wheel is as follows:

$$n = kU + C, \tag{1}$$

where n is the rotational speed, U is the input voltage of the motor ($U = -5\text{v} \sim +5\text{v}$), k and C are constants. The characteristics of two motors are different as regards real measurement. The characteristic curves of the left motor and the right motor are drawn in Fig. 2 and Fig. 3, respectively. The equation of the linear regression corresponding to the left motor is:

$$n_l = k_l U + C_l, \tag{2}$$

where n_l stands for the rotational speed of the left wheel, $k_l = 10.53472$, $C_l = -6.924367$. In the same way, the equation of the linear regression of the right motor is expressed as follows:

$$n_r = k_r U + C_r, \tag{3}$$

where n_r stands for the rotational speed of the right wheel, $k_r = 10.73956$, $C_r = -8.567838$. The angular velocity $\omega(t)$ of the AGV and the linear velocity $V_o(t)$ of two driving wheels'

https://doi.org/10.1017/S0263574799000740 Published online by Cambridge University Press

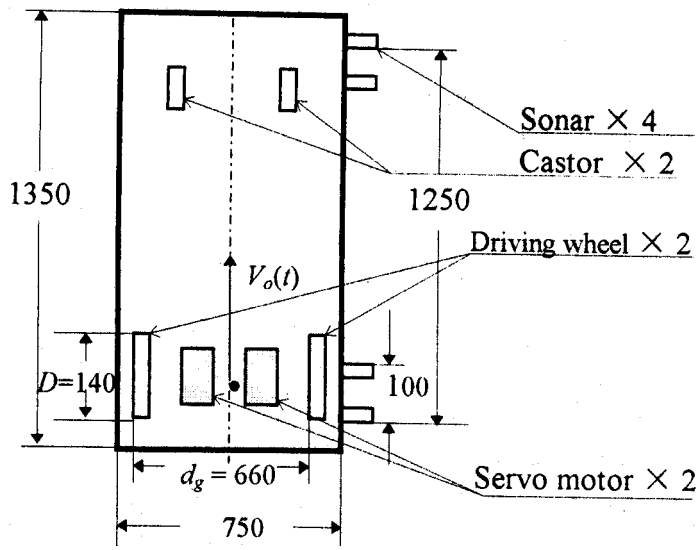


Fig. 1. The structure of the TIT-1 AGV.

midpoint (see Fig. 1) can be derived as follows:

$$\omega(t)=(n_l-n_r)D\pi/d_g, \tag{4}$$

$$V_o(t)=(n_1+n_r)D\pi/2. \tag{5}$$

Where D is the diameter of two driving wheels, d_g is the distance between two driving wheels (see Fig. 1). Substituting equations (2) and (3) into equations (4) and (5), we obtain

$$\omega(t)=(k_lU_l+C_l-k_rU_r-C_r)D\pi/d_g, \tag{6}$$

$$\begin{aligned} V_o(t)&=(k_lU_l+C_l+k_rU_r+C_r)D\pi/2\\ &=(k_lU_l+k_rU_r)D\pi/2+(C_l+C_r)D\pi/2. \end{aligned} \tag{7}$$

Where U_l and U_r, are the input voltages of the left motor and the right motor, respectively. On the basis of equation (7), we can show that $V_o(t)$ is constant when the following equation is satisfied.

$$U_g=(k_lU_l+k_rU_r)=\text{constant} \tag{8}$$

III THE DIGITAL FILTER

Two steps are taken to eliminate the disturbance from the door and the wrong readings from the specular reflection and accidental scattering.

(i) If $d_b\,(k)=d_{\max}$, then $d_b\,(k)=d_b\,(k-1)$,
If $d_f\,(k)=d_{\max}$, then $d_f\,(k)=d_f\,(k-1)$,

where $d_b\,(k)$ and $d_f\,(k)$ are the average readings of the back end sonars and the front sonars, respectively. $d_{\max}$ is the upper limit distance of sonars, which is taken as 150 centimeters in our experiments.

(ii) If $d_b\,(k)-d_b\,(k-1)\le\Delta d$, then $d_b\,(k)=d_b\,(k)$,
otherwise, if $d_b(k)-d_b(k-1)>\Delta d$, then $d_b(k)=d_b(k-1)$.
In the same way, if $d_f(k)-d_f(k-1)\le\Delta d$, then $d_f(k)=d_f(k)$,
otherwise, if $d_f(k)-d_f(k-1)>\Delta d$, then $d_f(k)=d_f(k-1)$.

Here, Δd is the biggest allowable deviations from two successive sampling distances of each sonar.

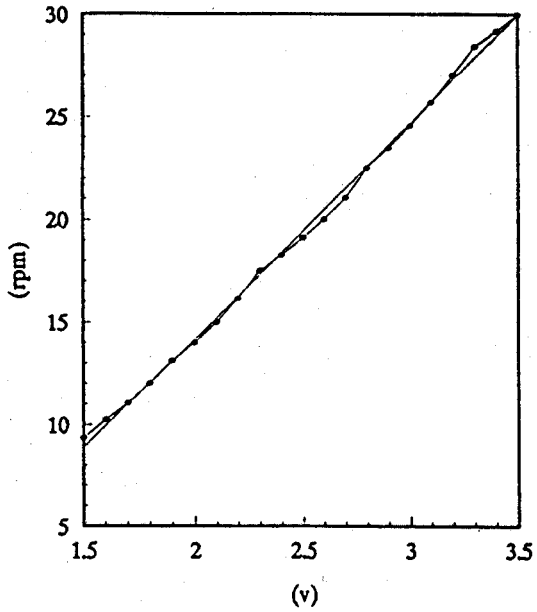


Fig. 2. The characteristic curve of the left motor.

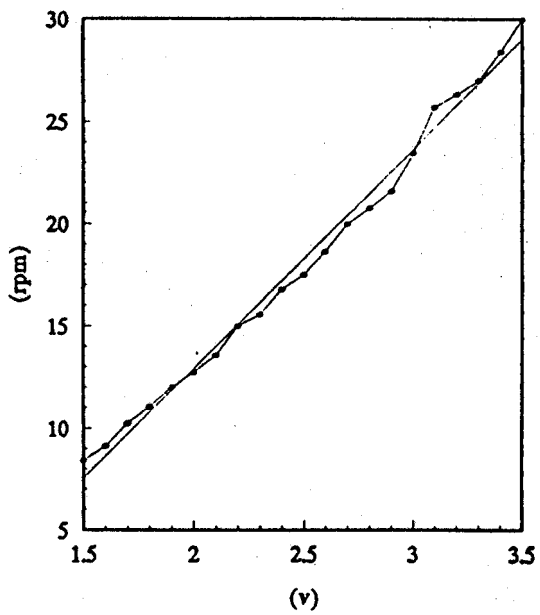


Fig. 3. The characteristic curve of the right motor.

https://doi.org/10.1017/S0263574799000740 Published online by Cambridge University Press

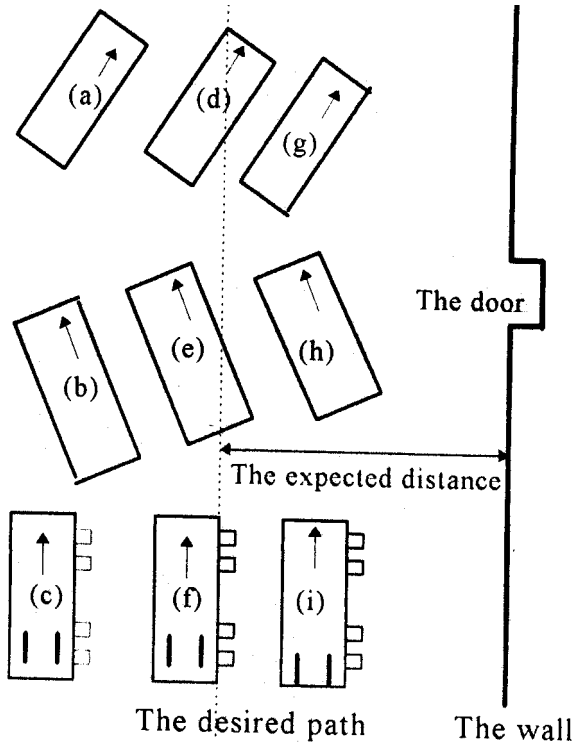


Fig. 4. Three kinds of moving states of the AGV.

IV CONTROL SCHEME

The AGV has three kinds of states during its motion (shown in Fig. 4). The first state includes (a), (b) and (c) where sonars' readings are all larger than the expected distance. The second state includes (g), (h) and (i), where readings are all smaller than the expected one. Fig. 4(d), (e), and (f) belong to the third state, where sonars' readings of one end are larger than or equal to the expected distance, but the readings of another end are smaller than or equal to the expected one.

IV.1. The structure of the controller

Fig. 5 shows the controller's structure, in which $y(k)$ is the output of the system, i.e. readings of four sonars. $\Delta d_{bf}(k)$ stands for the difference between $d_b(k)$ and $d_f(k)$. K_I is an integration coefficient. S_1 and S_2 are two choice switches controlled by two variables, i.e. $(d - d_b(k))$ and $(d - d_f(k))$, where d is the expected distance. When $(d - d_b(k))$ and $(d - d_f(k))$ are both very small (± 4 cm in our system) and have different signs, S_1 is switched to the I algorithm. Otherwise, S_1 is switched to the fuzzy control. In the course of fuzzy control, when $(d - d_b(k))$ and $(d - d_f(k))$ are both smaller than zero, the first kind of inference rule (rule I) is chosen. If $(d - d_b(k))$ and $(d - d_f(k))$ are both bigger than zero, the second kind of rule (rule II) is used. When $(d - d_b(k))$ and $(d - d_f(k))$ have different signs, the third kind of rule (rule III) is selected, k_1, k_2 and k_u are the scale factors of two inputs and one output, respectively. $\Delta u^*(k)$ is the quantization output of the fuzzy controller, $\Delta U(k)$ is the voltage increment of the motor at the kth sampling time; $U(k-1)$ is the voltage of the motor at the $(k-1)$th sampling time.

IV.2 The fuzzy control algorithm

The inputs of the fuzzy controller are two variables, i.e.

$$\Delta d_{bf}(k) = d_b(k) - d_f(k), \tag{9}$$

$$c_{bf}(k) = \frac{\partial[\Delta d_{bf}(k)]}{\partial t}. \tag{10}$$

The output of the fuzzy controller is $\Delta u^*(k)$. The voltage increment of the right motor at the kth sampling time is derived as follows:

$$\Delta U_r(k) = k_u \Delta u^*(k). \tag{11}$$

The voltages of the right motor and the left motor at the kth sampling time are given in equations (12) and (13), respectively.

$$U_r(k) = U_r(k-1) + \Delta U_r(k) \tag{12}$$

$$U_l(k) = (U_g - k_r \cdot U_r(k))/k_l \tag{13}$$

U_g is a constant in our experiment; $V_o(t)$ is also a constant.

(i) **Fuzzification.** $\Delta d_{bf}(k)$ is divided into five fuzzy subsets (see Fig. 6), which are expressed by NB, NS, Z, PS, and PB. Fig. 7 presents the membership functions and their corresponding labels of $c_{bf}(k)$. The membership functions of the controller's outputs are shown in Fig. 8.

(ii) **Fuzzy rules.** In our fuzzy controller, there are three kinds of inference rules, which correspond to three kinds of

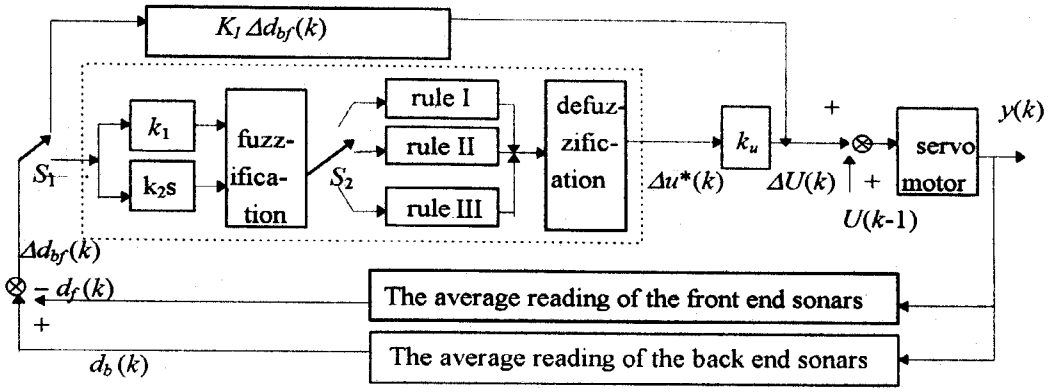


Fig. 5. The structure of the new FUZZY-I controller.

https://doi.org/10.1017/S0263574799000740 Published online by Cambridge University Press

moving states shown in Fig. 4. Each kind of inference rule includes 15 fuzzy rules. The first kind of intference rule (see Table I) corresponds to the first kind of the moving state (see Fig. 4(a), (b) and (c)), in which the readings of four sonars are all bigger than the expected distance. The basic ideas of the first kind of inference rule are: When the AGV moves toward the desired path (see Fig. 4(a)), the voltage increment of the right motor ($\Delta U_r(k)$) is positive or zero. Otherwise, if the AGV departs from or is parallel to the desired path (see Fig. 4(b) and (c)), $\Delta U_r(k)$ will be negative. The second kind of inference rule (see Table II) corresponds to the second kind of the moving state (see Fig. 4(g), (h) and (i)). The basic ideas of the second kind of inference rule are: When the AGV moves toward the desired path (see Fig. 4(h)), $\Delta U_r(k)$ will be negative or zero. Otherwise, if the

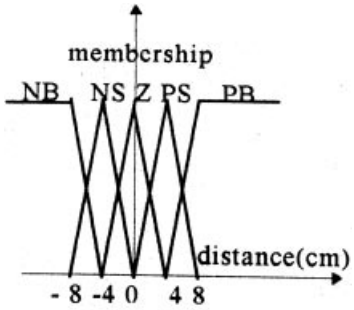


Fig. 6. The membership functions about $\Delta d_{bf}(k)$.

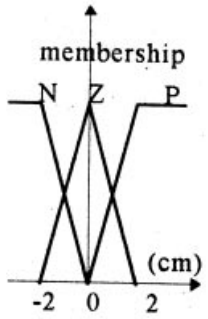


Fig. 7. The membership functions about $c_{bf}(k)$.

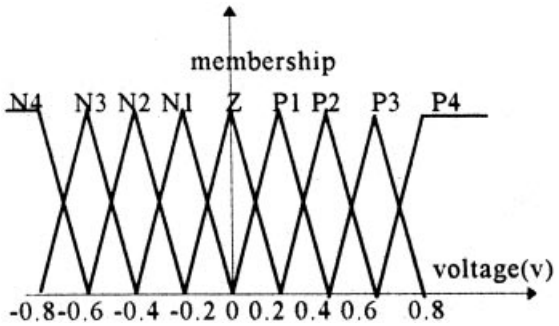


Fig. 8. The membership functions about the outputs of the controller.

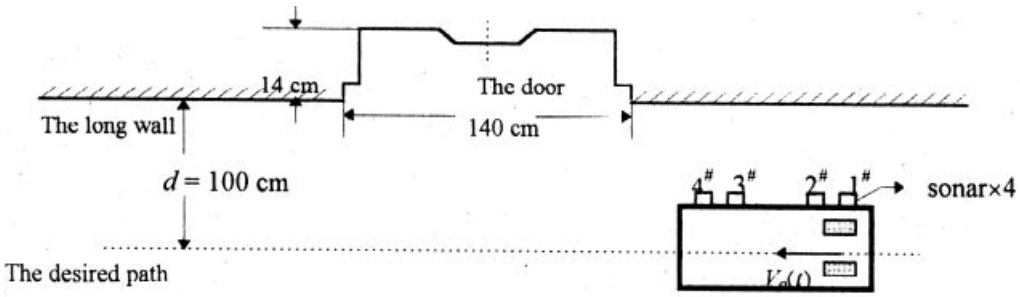


Fig. 9. The shape of the door and the moving direction of the TIT-1 AGV.

Table I. The first kind of inference rule

	1	2	3	4	5	6	7	8	9	10	11	12	13	14	15
$\Delta d_{bf}(k)$	PB	PB	PB	PS	PS	PS	N	N	N	NS	NS	NS	NB	NB	NB
$c_{bf}(k)$	P	Z	N	P	Z	N	P	Z	N	P	Z	N	P	Z	N
$\Delta\mu^*(k)$	P3	P2	P1	P1	Z	N1	Z	N1	N2	N1	N2	N3	N2	N3	N4

Table II. The second kind of inference rule

	1	2	3	4	5	6	7	8	9	10	11	12	13	14	15
$\Delta d_{bf}(k)$	PB	PB	PB	PS	PS	PS	N	N	N	NS	NS	NS	NB	NB	NB
$c_{bf}(k)$	P	Z	N	P	Z	N	P	Z	N	P	Z	N	P	Z	N
$\Delta\mu^*(k)$	P4	P3	P2	P3	P2	P1	P2	P1	Z	P1	Z	N1	N1	N2	N3

https://doi.org/10.1017/S0263574799000740 Published online by Cambridge University Press

Table III. The third kind of inference rule

	1	2	3	4	5	6	7	8	9	10	11	12	13	14	15
$\Delta d_{bf}(k)$	PB	PB	PB	PS	PS	PS	N	N	N	NS	NS	NS	NB	NB	NB
$c_{bf}(k)$	P	Z	N	P	Z	N	P	Z	N	P	Z	N	P	Z	N
$\Delta\mu^*(k)$	P3	P2	P1	P2	P1	Z	P1	Z	N1	Z	N1	N2	N1	N2	N3

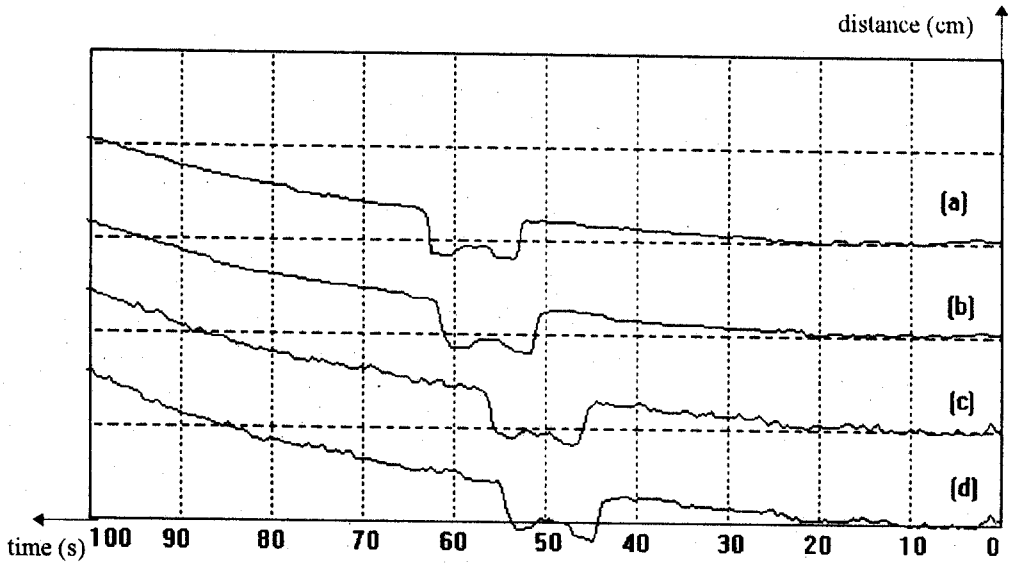


Fig. 10. The results of wall-following by the TIT-1 AGV without any control.

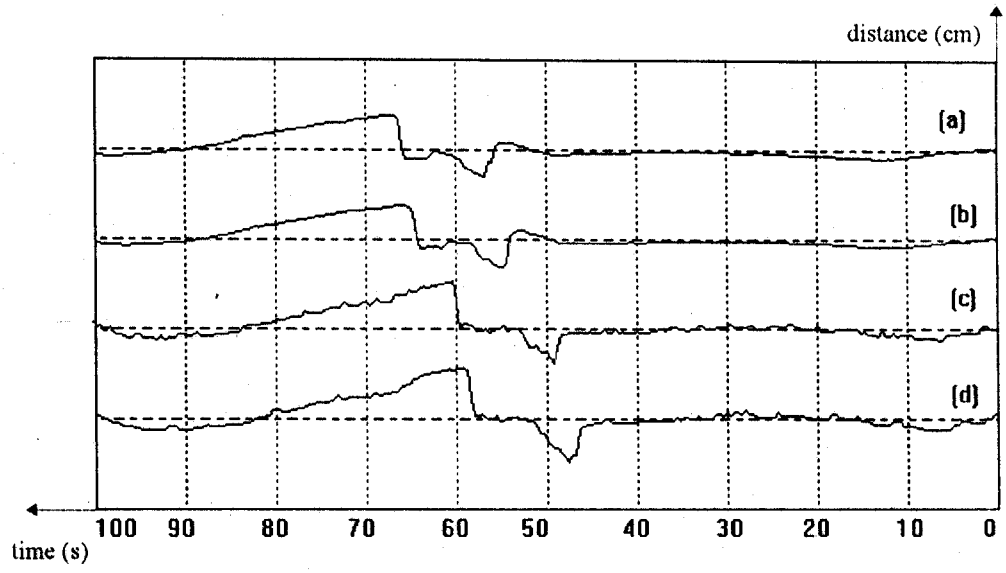


Fig. 11. The results of wall-following by the TIT-1 AGV only using the fuzzy controller.

https://doi.org/10.1017/S0263574799000740 Published online by Cambridge University Press

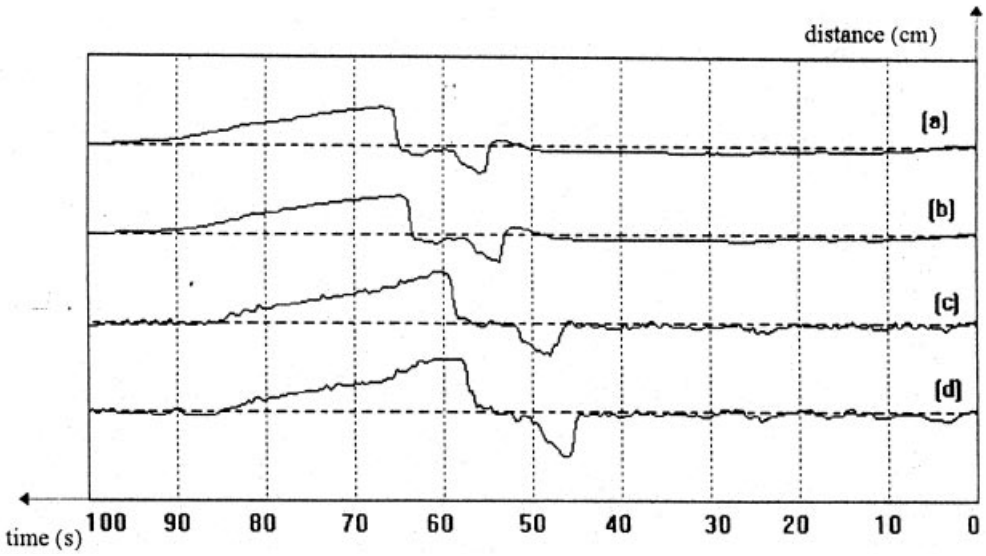


Fig. 12. The results of wall-following by the TIT-1 AGV using the fuzzy-I controller.

AGV departs from or is parallel to the desired path (see Fig. 4(g) and (i)), $\Delta U_r(k)$ will be positive. The third kind of inference rule is shown in Table III, whose basic ideas are: When $d_b(k)$ is bigger than $d_f(k)$ (see Fig. 4(d)), $\Delta U_r(k)$ will be positive. When $d_b(k)$ is smaller than or equal to $d_f(k)$ (see Fig. 4(e), (f)), $\Delta U_r(k)$ will be negative or zero.

$\Delta U_r(k)$ cannot be too large at each sampling time for each kind of inference rule. Otherwise, the angle between the moving direction of the AGV and the orientation of the long wall will be bigger than one half of the sonars' beam opening angle; this will result in wrong readings because of the phenomenon of specular reflection.

Note A (About switch S_2): In general, the inputs of the fuzzy controller corresponding to the wall-following problem of Fig. 4 have at least three variables, i.e.

$\Delta d_b(k) = [d - d_b(k)]$ (or $\Delta d_f(k) = [d - d_f(k)]$).

$\Delta d_{bf}(k) = [d_b(k) - d_f(k)]$, and $c_{bf}(k) = \dfrac{\partial[\Delta d_{bf}(k)]}{\partial t}$

(*three inputs also can be* $\Delta d_b(k)$, $\Delta d_f(k)$ *and* $\dfrac{\partial[\Delta d_b(k)]}{\partial t}$ $(or \dfrac{\partial[\Delta d_f(k)]}{\partial t})$).

Thus, the total number of the fuzzy rules is at least $3 \times 3 \times 3 = 27$ (i.e., each input is divided into three fuzzy subsets). If $\Delta d_{bf}(k)$ has five fuzzy subsets (like our fuzzy controller, see Fig. 6), the total number of the fuzzy rules will be at least $3 \times 5 \times 3 = 45$. The number of the fuzzy rules in our fuzzy controller is only $3 \times 5 = 15$ at each sampling time (because only one kind of inference rule is chosen at each sampling time). It can be seen that the computation of our method is relatively simple.

(iii) **Defuzzification.** The crisp output of the fuzzy controller is determined by the weighted mean of the centre gravity; the result is given as follows:

$$\Delta u(k) = \sum_{i=1}^{15} \mu(i) \bullet x(i) / \left(\sum_{i=1}^{15} \mu(i) \right). \qquad (14)$$

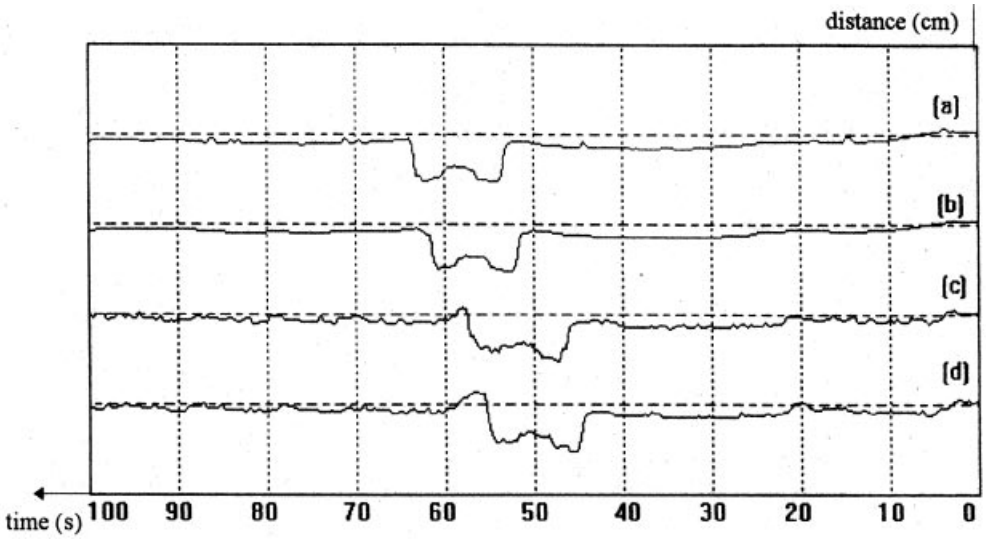


Fig. 13. The results of wall-following by the TIT-1 AGV using the fuzzy controller and the digital filter.

https://doi.org/10.1017/S0263574799000740 Published online by Cambridge University Press

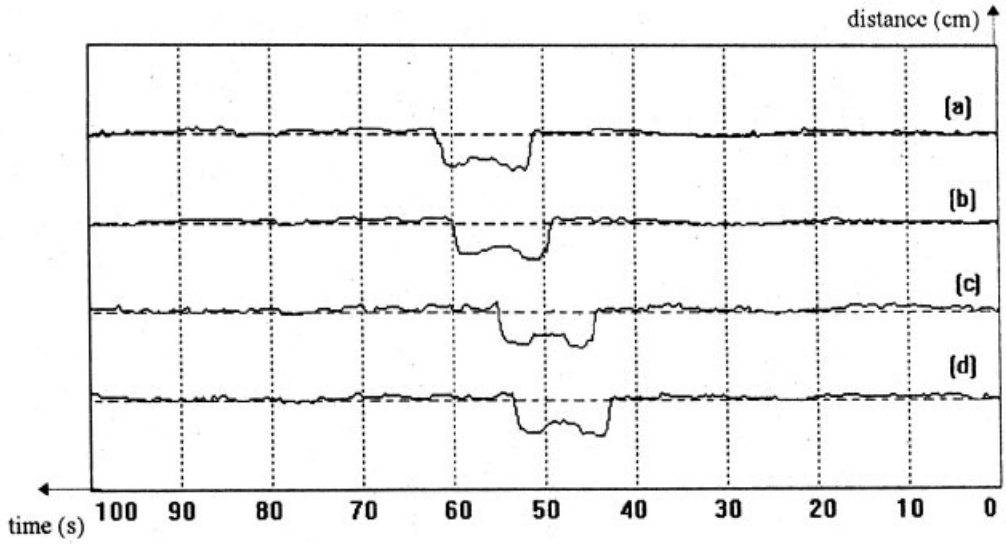


Fig. 14. The results of wall-following by the TIT-1 AGV using the fuzzy-I controller and the digital filter.

Here, $\mu(i)(0 \le \mu(i) \le 1)$ is the activation strength of each rule $i(i=1,2,\ldots,15)$, $x(i)$ is the center value of the horizontal coordinate of the membership function corresponding to the output of rule i.

IV.3 The integration (I) *regulator*

The I algorithm is written as follows:

$$\Delta U_r(k) = K_I \Delta d_{bf}(k), \tag{15}$$

$$U_r(k) = U_r(k-1) + \Delta U_r(k). \tag{16}$$

Here, K_I is the integration coefficient. $U_I(k)$ is calculated out by equation (13).

Note B (About switch S_1): In general, a two-dimension fuzzy control (i.e. there are two input varaibles, the error and its change with time) only has an effect similar to the proportional and differential control (i.e. PD control). Thus, a two-dimension fuzzy control has a good dynamic control performance, but it usually has a steady-state deviation due to a lack of integration (I) control. To eliminate remaining errors, an I regulator is used when $(d - d_b(k))$ and $(d - d_f(k))$ have different signs and the absolute value of $\Delta d_{bf}(k)$ is smaller than a threshold (4 cm in our experiments).

V EXPERIMENTS

Four Polaroid sonars are used in our experiments; the effective range of four sonars is from 40 centimeters to 1.5 meters, the resolution is 0.5 centimeters. The distance between every two sonars is shown in Fig. 1. The beam-opening angle of each sonar is about 30°. The range data is processed by an Intel 8051 single-chip microcomputer; the control algorithm is completed on an industrial 386. The rotational speeds of two driving motors are also controlled by a single-chip computer system. Communication is provided via RS232 serial lines. Four sonars are initiated successively to prevent the phenomenon of "crosstalk" between sonars. The sampling period is 0.4 seconds. The software is written by a combination of *MCS-51* assembly language and *C* language. The linear velocity $V_o(t)$ is a constant (10 meters/minute) in the process of wall-following, i.e. the control algorithm guarantees that equation (8) is satisfied (in our experiment, $U_g = 5$). The experimental environment is a 15-meter-long wall (see Fig. 9).

The moving direction of the AGV is from right to left. The initial state of the AGV is parallel to the long wall. Figs. 10 to Fig. 14 are the experimental results, where curve (a) to curve (d) are drawn using four sonars' readings (i.e. the readings of sonar $1^{\#}$, $2^{\#}$, $3^{\#}$, and $4^{\#}$, respectively; see Fig. 9). In the vertical axis, each lattice stands for 30 cm. The concave in each curve results from the door. Fig. 10 shows the results of wall-following by the TIT-1 AGV without any control. The trajectory of the AGV departs from the desired path after 10 seconds because of different characteristics of two motors and wheel slippage. The biggest errors between the readings of four sonars and the expected distance are about 48 cm for the whole course of following the 15-meter-long wall (see the curve (d) in Fig. 10). The results of wall-following only by using the fuzzy controller are shown in Fig. 11. When the AGV moves near to the door, the readings of the front sonars (i.e. sonar $4^{\#}$ and $3^{\#}$, see Fig. 9) become suddenly large. Though the AGV does not depart from the desired path, the fuzzy controller has to reduce the voltage on the right motor immediately. Thereby, the AGV moves toward the door till the two back sonars (i.e. sonar $2^{\#}$ and $1^{\#}$, see Fig. 9) also can "find" the door. When two front sonars cannot "find" the door and two back sonars still can "find" it, the fuzzy controller will have to increase the voltage on the right motor till the two back sonars cannot also "find" the door. After the AGV moves away from the door, the fuzzy controller will gradually regulate the moving direction of the AGV to make it move along the desired path. Fig. 12 presents the results by using the fuzzy-I controller. Comparing Fig. 12 with Fig. 11, we can see that the AGV has less oscillation in Fig. 12 because of the function of the I controller, but it also has bad control performance near the door. Fig. 13 gives the results by using the fuzzy controller and the digital filter, showing an obvious improvement near the door because of the function

https://doi.org/10.1017/S0263574799000740 Published online by Cambridge University Press

of the digital filter. Fig. 14 shows the results by using the fuzzy-I controller and the digital filter, in which the errors between the readings of four sonars and the expected distance are within ±2 cm during the entire process. The shape of the door can be distinctly seen in Fig. 13 and Fig. 14 owing to the function of the digital filter. From Figs 10 to 14, we can conclude that the dynamic and steady performances of the AGV having the I algorithm are better than those without the I algorithm; in the same way, the performances having the digital filter are better than that without it.

VI CONCLUSION

In this paper, four Polaroid sonars are used to measure the distance between the right side of our TIT-1 AGV and the long wall. A digital filter is used to get rid of the disturbance from the door and wrong readings due to the specular reflection and accidental scattering of sonars. To obtain good dynamic and steady performances, a new compound fuzzy-I control algorithm is used by us. The fuzzy controller consists of three kinds of fuzzy inference rules used to adjust three kinds of moving states of the AGV. The I algorithm is used to eliminate remaining errors. Our methods have been verified by following a 15 meter-long wall with a door by our TIT-1 AGV. The results show good performance with errors of ±2 cm from the expected distance to the wall.

References

1. C.J. Harris, D. Charnley, "Intelligent autonomous vehicle: recent progress and central research issues", *Computing & Control Engineering J.* 164–171 (July, 1992).
2. Transitions Research Corp., Helpmate preliminary specification (1988).
3. Mark B. Kadonoff, "Ultrasonic wall-following controller for mobile robots" *SPIE* **1195** Mobile Robots IV 391–401 (1989).
4. P. van Turennout, G. Honderd, "Following a wall with a mobile robot using ultrasonic sensors", *Proc. of the 1992 IEEE/RSJ Int. Conf. on Intelligent Robots and Systems*, Raleigh, NC (July, 7–10, 1992), pp. 1451–1456.

https://doi.org/10.1017/S0263574799000740 Published online by Cambridge University Press